

1

Supplementary Material

2

for

3

Correction and new understanding of reactivity for illuminated

4

tungsten trioxide under dark: Antecedents and consequences of

5

photo-storage electrons triggering Fenton reactions

6

Hao Huang, Hui-Long Wang*, Wen-Feng Jiang*

7

School of Chemistry, Dalian University of Technology, Dalian 116023, China

8

9

10

11

12 Corresponding author: hlwang@dlut.edu.cn (H.-L. Wang)

13 dlutjiangwf@163.com (W.-F. Jiang)

14

15

16

17

18 Number of pages: 16

19 Number of figures: 11

20 Number of tables: 3

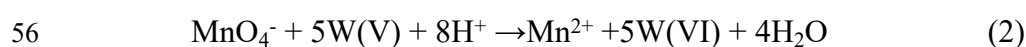
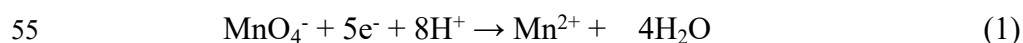
Contents

21		
22	1. Experimental procedure	-3-
23	Text S 1.1. Quantitative experiments on stored electrons in LP-t min samples	-3-
24	Text S 1.2. The oxidation experiments of I ⁻ for different catalysts.....	-3-
25	Text S 1.3. Theoretical calculation details	-4-
26	2. Results and Discussion	-5-
27	Figure S1. SEM image of h-WO ₃ •0.46H ₂ O	-5-
28	Figure S2. The refined crystal structure unit of h-WO ₃ •0.46H ₂ O	-6-
29	Figure S3. Photographs of different illuminated h-WO ₃ •0.46H ₂ O samples.....	-6-
30	Figure S4. Reflectance of different illuminated h-WO ₃ •0.46H ₂ O samples.....	-6-
31	Figure S5. Reflectance of different illuminated h-WO ₃ •0.46H ₂ O samples.....	-7-
32	Figure S6. UV–vis spectra and standard curves of KMnO ₄ solution.	-7-
33	Figure S7. Schematic representation of the reduction process of MnO ₄ ⁻	-7-
34	Figure S8. TOC removal for DNBP degradation by different reaction systems ...	-8-
35	Figure S9. The TOC removal and trapping experiments of reactive species through	
36	DNBP degradation process for LP-80 min through different cycle times	-8-
37	Figure S10. XRD pattern of the sample before and after DFR process	-9-
38	Figure S11. Mass spectra (MS) of intermediates during the DFR process	-10-
39	Table S1. Different round-the-clock photocatalysts based on stored electrons in WO ₃	
40	for organic contaminants degradation under dark condition.	-12-
41	Table S2. Results of the refinement data of h-WO ₃ •0.46H ₂ O in the Space Group	
42	<i>P6/mmm</i>	-13-
43	Table S3. Intermediates of DNBP in illuminated h-WO ₃ •0.46H ₂ O/H ₂ O ₂ system-	13-
44	2. Reference	-15-
45		
46		
47		
48		
49		

50 1. Experimental Procedures

51 1.1. Quantitative experiments on stored electrons in LP-t min 52 samples.

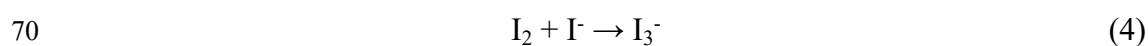
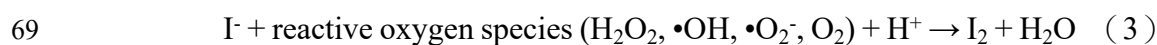
53 KMnO_4 as a selective probe reagent for the stored electrons (W(V)) trapping through
54 Eq. (1) or (2):



57 Firstly, KMnO_4 solution with different concentrations (5, 50, 100, 120, 150, 200 ppm)
58 were prepared at pH of 1 (The solvent was the 0.05 M/L H_2SO_4 solution). Then, the
59 reduction experiments of KMnO_4 were carried out following certain steps: 20 mg of
60 LP-t min was added into 30 ml KMnO_4 solution with certain concentration under
61 stirring conditions in dark. After 2 h, 3 mL of suspension were withdrawn, centrifuged
62 and the supernatant was analyzed for evolution in concentration of KMnO_4
63 spectrophotometrically at λ_{max} of 525 nm. Finally, based on the consumption amount of
64 KMnO_4 , the content (mmol/g) of W(V) in LP-t min sample is calculated to obtain the
65 concentration (mmol/g) of stored electrons in the catalyst.

66 1.2. The oxidation experiments of I⁻ for different catalysts.

67 I_3^- as a selective probe reagent for existence of reactive oxygen species (H_2O_2 , $\bullet\text{OH}$,
68 $\bullet\text{O}_2^-$, O_2) through Eq. (3) and (4)



71 150 μL of 10 wt. % H_2O_2 was poured into 30 ml deionized water under magnetic
72 stirring. After 10 min, 30 mg catalyst was added into above solution. After 1 h of
73 continuous stirring, 5 mL of suspension were withdrawn, centrifuged and the
74 supernatant was obtained. Subsequently, 10 μL of $(\text{NH}_4)_2\text{MoO}_4$ solution with
75 concentration of 10 $\mu\text{M/L}$ and 0.5 ml of KI solution with concentration of 100 mM/L
76 were added into the supernatant. The solution was stirred for 5 minutes and then
77 analyzed for evolution in concentration of I_3^- spectrophotometrically at λ ($\lambda_1 = 287$ nm,
78 $\lambda_2 = 350$ nm).

79 **1.3. Theoretical calculation details.**

80 In this work, the adsorption process of H_2O_2 on the (001) surface of h- WO_3 hydrate
81 were studied in the CASTEP module. The Perdew-Burke-Ernzerhof (PBE) functional
82 based on the generalized-gradient approximation (GGA) was used to described the
83 exchange and correlation interactions between atoms. The cutoff energy of the plane
84 wave was 300 eV and the tolerance for accepting convergence of the total energy per
85 atom was 10^{-5} eV atom $^{-1}$. Moreover, the Brillouin zone was sampled using a suitable
86 Γ point. The adsorption binding energy E_{ads} was calculated according to Eq. (5).

$$87 \quad E_{ads} = E_{total} - E_{adsorbate} - E_{adsorbent} \quad (5)$$

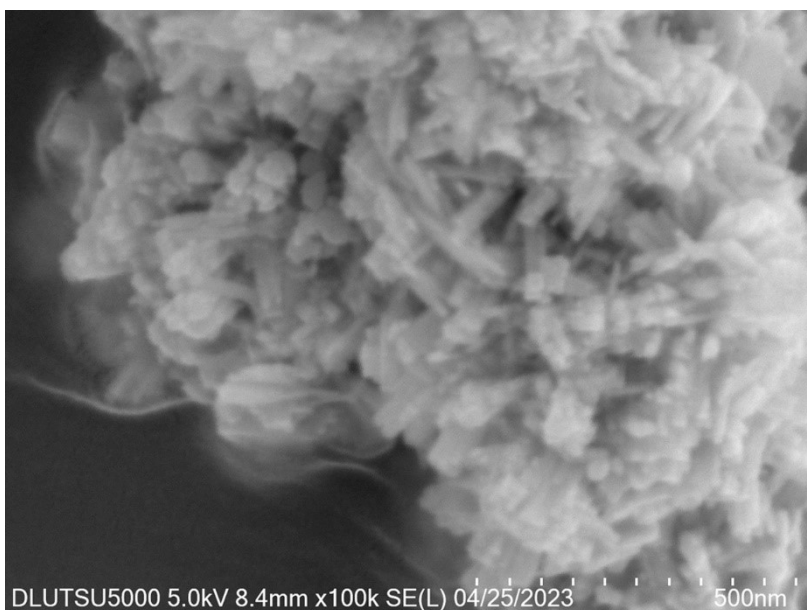
88 where E_{total} , $E_{adsorbate}$ and $E_{adsorbent}$ correspond to the total energies of the system,
89 antibiotics, and adsorbents, respectively.

90 Molecular dynamics (MD) simulations were used to study the adsorption behavior of
91 H_2O_2 molecule on the (001) surface of h- WO_3 hydrate. The computational model was
92 composed by the h- WO_3 hydrate (3×3) super cell, H_2O_2 solution slab and vacuum slab

93 (30 Å). Before calculation, the constructed system was geometrically optimized. The
94 condensed phases were simulated using the force field UNIVERSAL. The Ewald
95 summation technique was used to set bonded and unbonded terms as atom-based
96 summations. The Nasal thermostat was used to perform constant temperature molecular
97 dynamics simulations at 298 ± 10 K with a time step of 1.0 fs and a simulation time of
98 1000 ps.

99 Quantum chemical calculations were performed using Gaussian 09 program with DFT
100 algorithm to optimize the structure of DNBP at the B3LYP/6-31G (d, p) level. The
101 wave function analysis was carried out using the Multiwfn program to obtain the
102 frontier molecular orbitals (the highest occupied molecular orbits (HOMO), the lowest
103 unoccupied molecular orbits (LUMO), surface electrostatic potential (ESP)) and Fukui
104 indices of DNBP molecule.

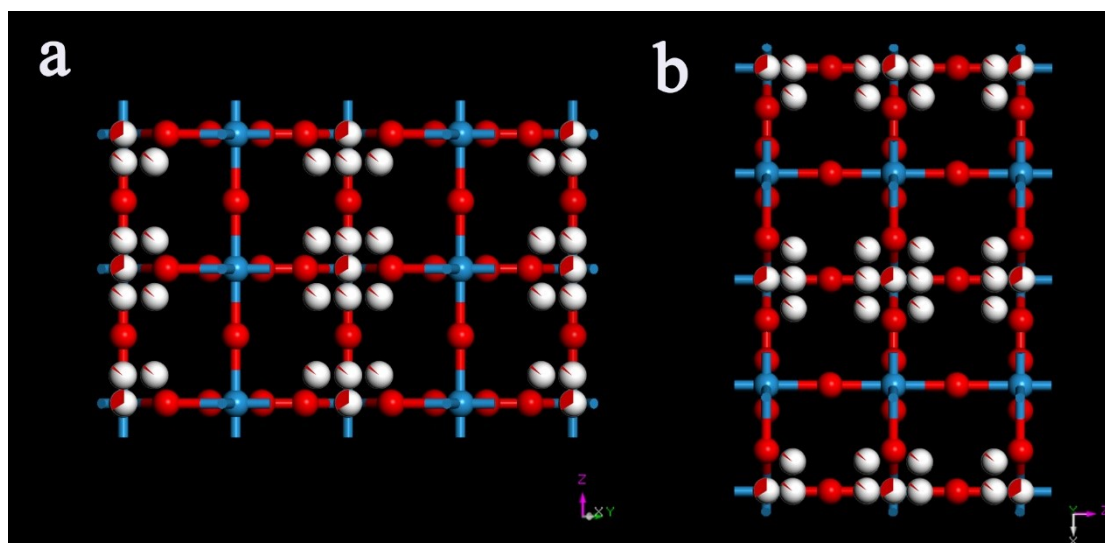
105 **2. Results and Discussion**



106
107 **Figure S1.** SEM image of $h\text{-WO}_3 \cdot 0.46\text{H}_2\text{O}$.

108

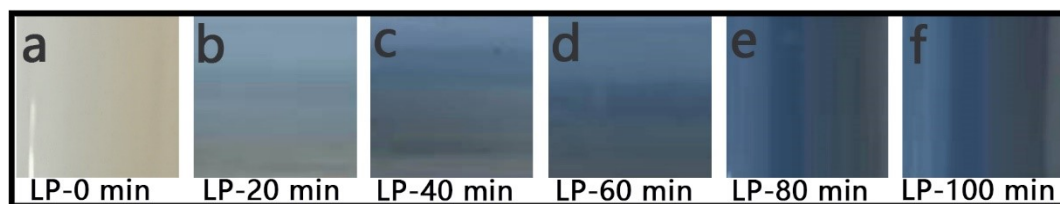
109



110

111 **Figure S2.** The refined crystal structure unit of $h\text{-WO}_3\cdot 0.46\text{H}_2\text{O}$ viewed toward (a) yz
112 plane and (b) xz plane.

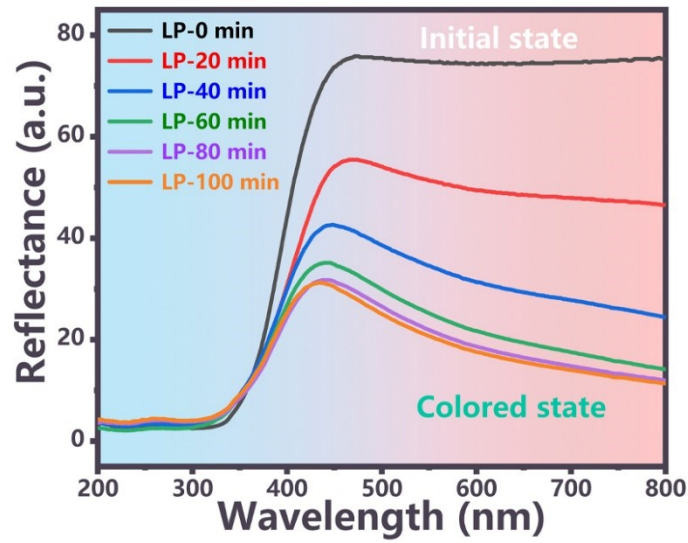
113



114

115 **Figure S3.** Optical photographs of different illuminated $h\text{-WO}_3\cdot 0.46\text{H}_2\text{O}$ samples.

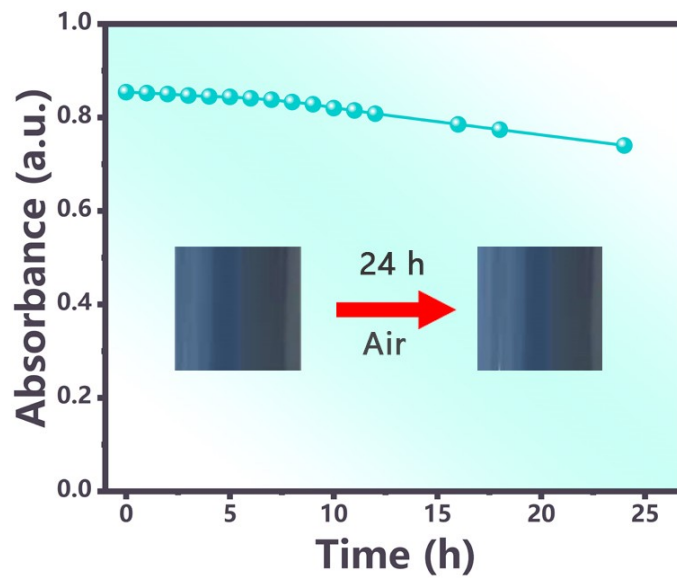
116



117

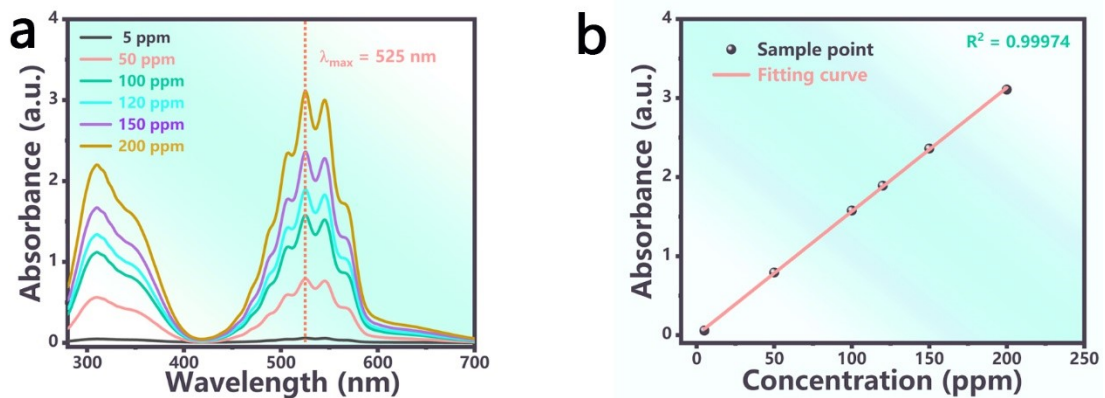
118 **Figure S4.** Reflectance spectra of different illuminated $h\text{-WO}_3\cdot 0.46\text{H}_2\text{O}$ samples.

119



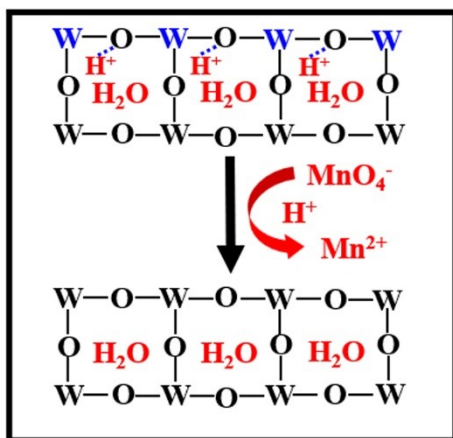
120

121 **Figure S5.** Reflectance spectra of different illuminated $h\text{-WO}_3\cdot 0.46\text{H}_2\text{O}$ samples.

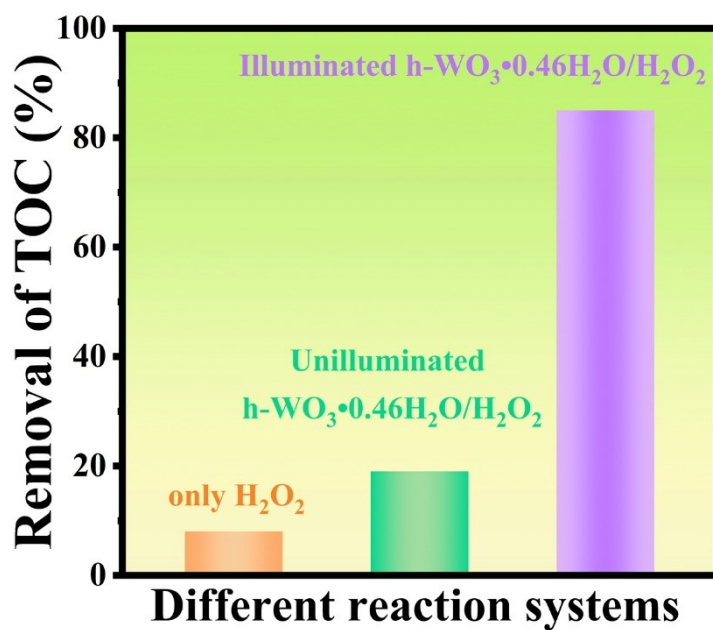


122

123 **Figure S6.** (a) UV-vis absorbance spectra of KMnO_4 solution with different
 124 concentration and (b) standard curve based on the absorbance at $\lambda_{max} = 525 \text{ nm}$.

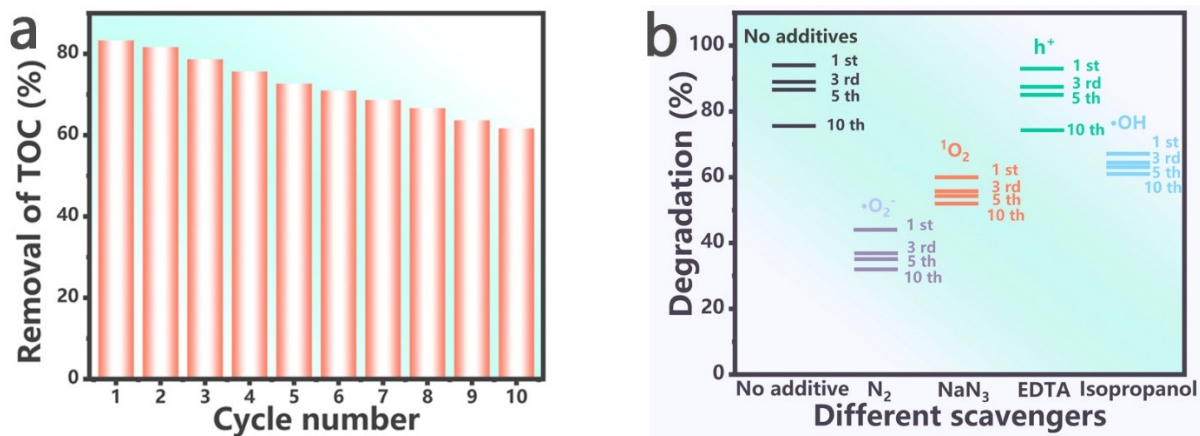


125
 126 **Figure S7.** Schematic representation of the reduction process of MnO_4^- among
 127 illuminated $\text{h-WO}_3 \cdot 0.46\text{H}_2\text{O}$.



128
 129 **Figure S8.** TOC removal for DNB degradation by different reaction systems.

130

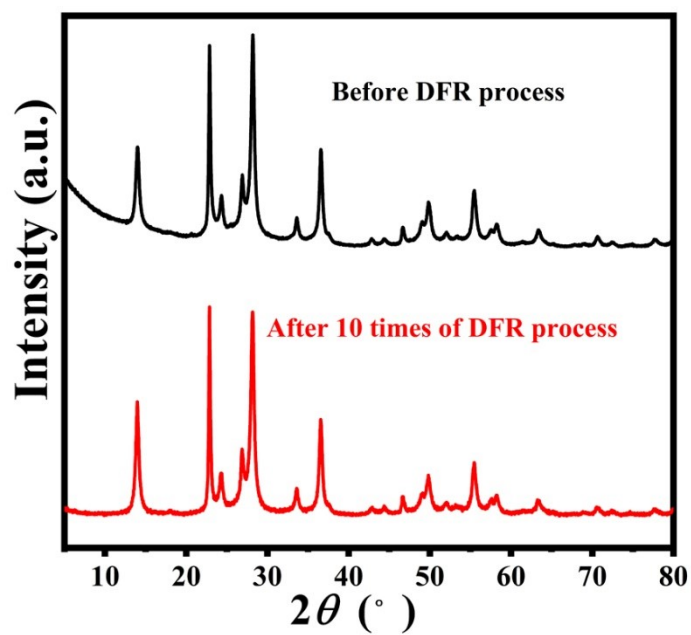


131

132 **Figure S9.** (a) The TOC removal and (b) trapping experiments of reactive species

133 through DNBP degradation process for LP-80 min through different cycle times.

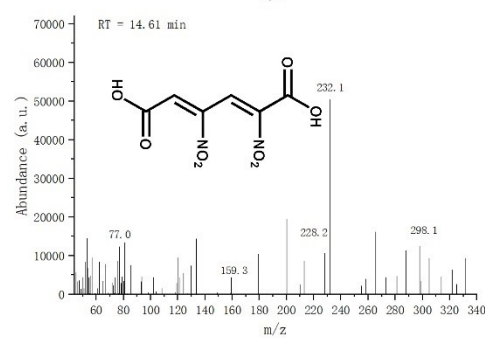
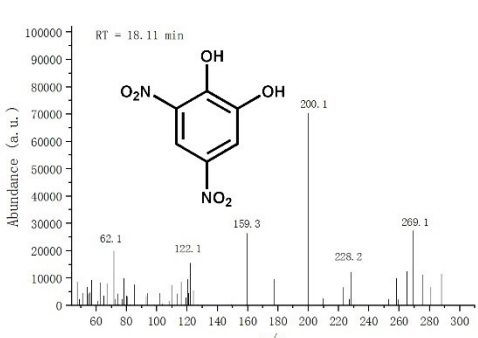
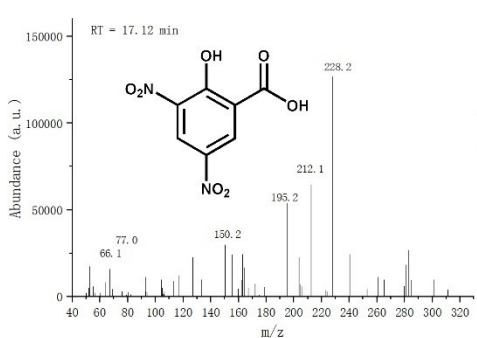
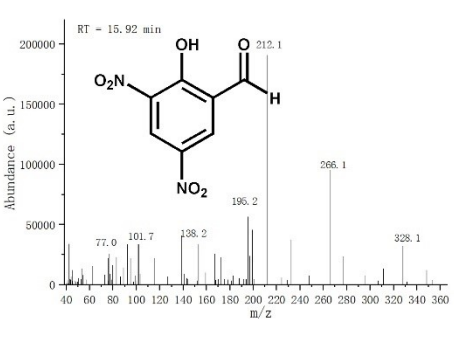
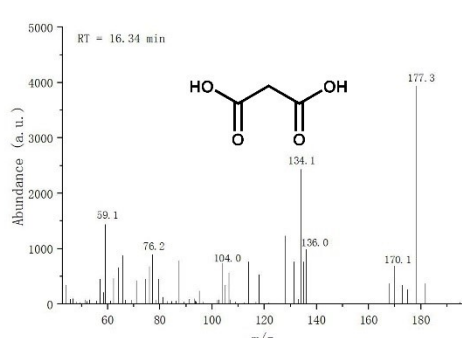
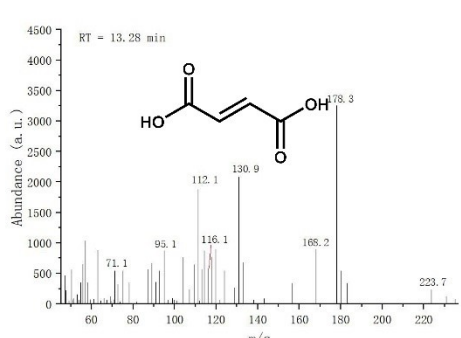
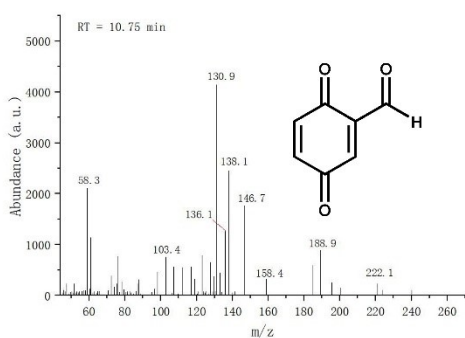
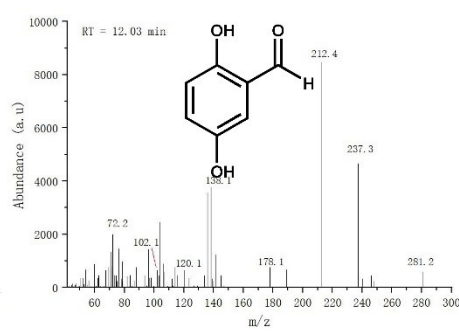
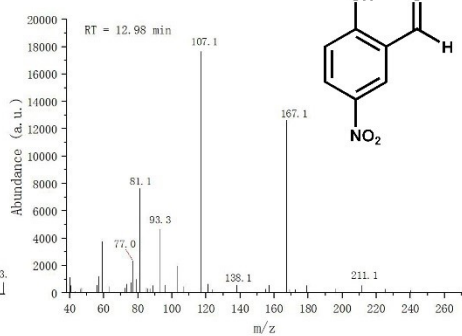
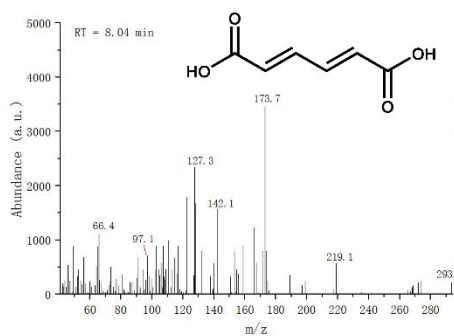
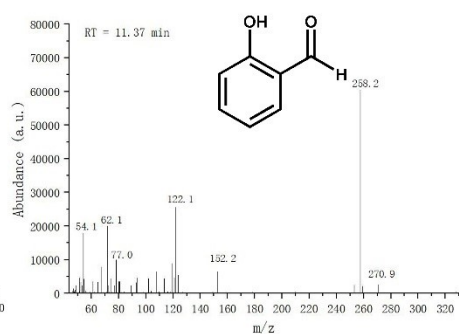
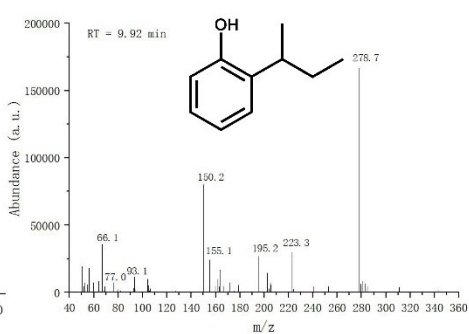
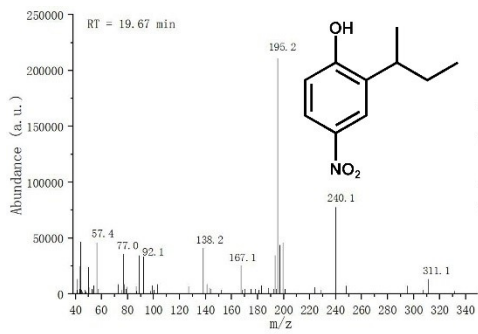
134



135

136 **Figure S10.** The XRD pattern of illuminated h-WO₃•0.46H₂O before and after 10 times

137 of DFR process.



139 **Figure S11.** Mass spectra (MS) of intermediates during the process of DNBP
140 degradation among illuminated h-WO₃•0.46H₂O/H₂O₂ system.

141

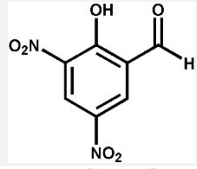
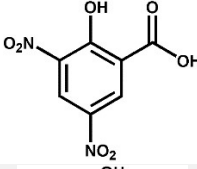
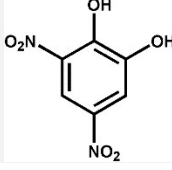
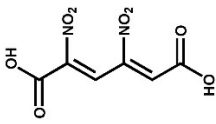
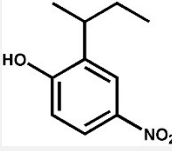
Table S1. Different round-the-clock photocatalysts based on stored electrons in WO₃ for organic contaminants degradation under dark condition.

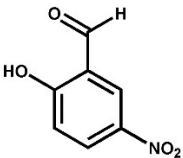
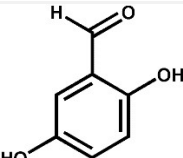
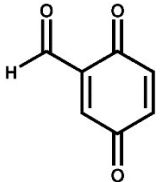
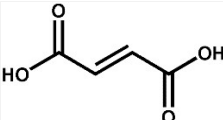
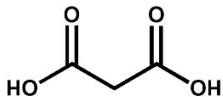
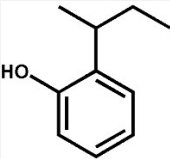
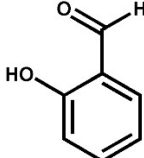
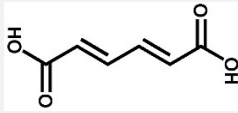
Photocatalysts	Pollutants	Light source	Illumination reaction time (charging)	Dark reaction time (discharging)	Active species in the dark reaction	References
Spray dried TiO ₂ /WO ₃ heterostructure	Methylene blue	UV	40 min	30 min	•OH	1
WO ₃ /TiO ₂ hollow microsphere composites	Methyl orange	Vis	40 min	40 min	•OH	2
Pt: TiO ₂ /WO ₃ photocatalyst	Methanol	Vis	2 h	6 h	•OH	3
Dual-phase TiO ₂ /WO ₃	Methanol	stimulated solar light	2 h	6 h	•O ₂ ⁻	4
WO ₃ /g-C ₃ N ₄ composite	Rhodamine B	Vis	1 h	8 h	•OH	5
Pt-TiO ₂ /WO ₃ hybrid material	Methylene blue	UV/Vis	30 min	60 min	•OH	6
n-MoS ₂ /p-WO ₃ based diode catalyst	Methylene blue	-	-	-	•OH	7
Mg-ZnO/WO ₃ QDs/GO	Rhodamine B	UV/Vis	6 h	2 h	•O ₂ ⁻	8

Table S2. Results of the refinement data of h-WO₃·0.46H₂O in the Space Group P6/mmm.

	Atom	x	y	z	Occupancy	B	Site	Symmetry
1	W1	0.50000	0.00000	0.00000	1.000	1.381	3f	mmm
2	O1	0.38380	0.19190	0.00000	1.000	1.164	6l	mm2
3	O2	0.50000	0.00000	0.50000	1.000	1.858	3g	mmm
4	O3	0.00000	0.00000	0.00000	0.402	2.500	1a	6/mmm
5	O4	0.13990	0.13990	0.20979	0.027	4.000	12n	...m

Table S3. Intermediates of DNBP in illuminated h-WO₃·0.46H₂O/H₂O₂ system.

The series number of intermediates	Formula	m/z	Structure	Retention time (min)
1	C ₇ H ₄ N ₂ O ₆	212		15.92
2	C ₇ H ₄ N ₂ O ₇	228		17.12
3	C ₆ H ₄ N ₂ O ₆	200		18.11
4	C ₆ H ₄ N ₂ O ₈	232		14.61
5	C ₁₀ H ₁₃ NO ₃	195		19.67

6	$C_7H_5NO_4$	167		12.98
7	$C_7H_6O_3$	138		12.03
8	$C_7H_4O_3$	136		10.75
9	$C_4H_4O_4$	116		13.28
10	$C_3H_4O_4$	104		16.34
11	$C_{10}H_{14}O$	150		9.92
12	$C_7H_6O_2$	122		11.37
13	$C_6H_6O_4$	142		8.04

3. Reference

- [1] H. Khan, M. G. Rigamonti, G. S. Patience, D. C. Boffito, Spray dried TiO₂/WO₃ heterostructure for photocatalytic applications with residual activity in the dark. *Appl. Catal. B: Environ.*, 2018, **226**, 311-323.
- [2] Y. Li, L. Chen, Y. Guo, X. Sun, Y. Wei, Preparation and characterization of WO₃/TiO₂ hollow microsphere composites with catalytic activity in dark. *Chem. Eng. J.*, 2012, **181-182**, 734-739.
- [3] M. Mokhtarifar, D. T. Nguyen, M. Sakar, M. Pedferri, M. Asa, R. Kaveh, M. V. Diamanti, T.-O. Do, Mechanistic insights into photogenerated electrons store-and-discharge in hydrogenated glucose template synthesized Pt: TiO₂/WO₃ photocatalyst for the round-the-clock decomposition of methanol. *Mater. Res. Bull.*, 2021, **137**, 111203.
- [4] M. Mokhtarifar, D. T. Nguyen, M. V. Diamanti, R. Kaveh, M. Asa, M. Sakar, M. Pedferri, T.-O. Do, Fabrication of dual-phase TiO₂/WO₃ with post-illumination photocatalytic memory. *New. J. Chem.*, 2020, **44**, 20375-20386.
- [5] J. Du, Z. Wang, Y. Li, R. Li, X. Li, K. Wang, Establishing WO₃/g-C₃N₄ Composite for “Memory” Photocatalytic Activity and Enhancement in Photocatalytic Degradation. *Catal. Lett.*, 2019, **149**, 1167-1173.
- [6] H. Khan, M. G. Rigamonti, D. C. Boffito, Enhanced photocatalytic activity of Pt-TiO₂/WO₃ hybrid material with energy storage ability. *Appl. Catal. B: Environ.*, 2019, **252**, 77-85.
- [7] W. L. Kebede, D.-H. Kuo, K. E. Ahmed, H. Abdullah, Dye degradation over the multivalent charge- and solid solution-type n-MoS₂/p-WO₃ based diode catalyst under dark condition with a self-supporting charge carrier transfer mechanism. *Adv. Powder. Technol.*, 2020, **31**, 2629-2640.

[8] H. Zhao, Q. Fang, C. Chen, Z. Chao, Y. Tsang, Y. Wu, WO₃ Quantum Dots Decorated GO/Mg-doped ZnO Composites for Enhanced Photocatalytic Activity under Nature Sunlight. *Appl. Organomet. Chem.*, 2018, **32**, e4449.